Supporting Information

Self-assembly of the Imidazolium Surfactant in the Aprotic Ionic Liquids. The Anion Effect of Aprotic Ionic Liquids

Pan Yue,[a] Zhao Chunhua,[b,c] Wang Ruirui,[a] Zhu Mingjie, [a] Zhuang Wenchang,[a] Li Qintang*[a]

[a] School of Materials and Chemical Engineering, Xuzhou University of Technology, Xuzhou 221018, P. R. China

[b] State Key Laboratory of Offshore Oil and Gas Exploitation, Beijing 100028, P. R. China

[c] CNOOC Research Institute Ltd., Beijing 100028, P. R. China

ORCID:

Yue Pan: 0000-0001-9972-6917

Qintang Li: 0000-0001-6311-4281

Corresponding author:

Qintang Li

E-mail: liqintangwind@sina.com

^{1}H NMR Characterization

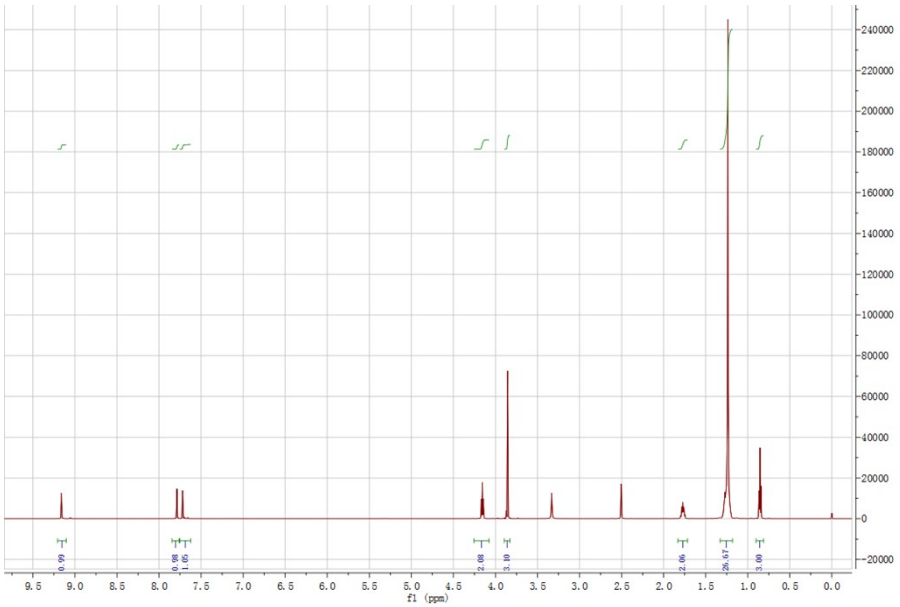

Fig. S1 ^{1}H NMR spectrum of C_{16}mimBr.

C_{16}mimBr (DMSO, 600 MHz) 0.83-0.88 (3H), 1.18-1.30 (26H), 1.73-1.82 (2H), 3.83-3.89 (3H), 4.10-4.20 (2H), 7.70-7.75 (1H), 7.76-7.80 (1H), 9.10-9.20 (1H).

Calculation of surface adsorption parameters

The surface parameters, such as the effectiveness of γ reduction (Π_{CMC}), the surface excess at the air/IL interface (Γ_{max}), the minimum area per surfactant molecule adsorbed at the surface (A_{min}) and the Gibbs free energy of micellization (ΔG_m), can be calculated according to equations S1-S4 below, where γ_0 and γ_{CMC} are surface tensions of the pure solvent and the solution at CMC, respectively.

$$\Pi_{CMC} = \gamma_0 - \gamma_{CMC} \qquad \text{(S1)}$$

$$\Gamma_{max} = -\frac{1}{RT}\left(\frac{d\gamma}{d\ln C}\right) \qquad \text{(S2)}$$

$$A_{min} = \frac{1}{N_A \Gamma_{max}} \qquad \text{(S3)}$$

$$\Delta G_m = RT \ln X_{CMC} \qquad \text{(S4)}$$

SAXS analysis of Micelles

The SAXS curves of micelles were fitted with the SASfit software (version 0.94.7). The scattering of ellipsoid could be expressed as,

$$I(q,a,\varepsilon) = (\frac{4}{3}\pi a^3 \Delta\eta)^2 \int_0^{\frac{\pi}{2}} K^2(q,a\sqrt{\varepsilon^2 cos^2\theta + sin^2\theta}) sin\theta d\theta \quad \text{(S5)}$$

where a is the radius of the rotational axis, ε is ratio between radius of the semi-principle axes and equatorial axis.

The hard sphere structure factor with Percus-Yevick closure relation and decoupling approach was adopted for the interaction between micelles. The structure factor of hard sphere could expressed as,

$$S(q,R_{HS},f_q) = \frac{1}{1 + 24 f_q \frac{G(f_q,R_{HS}q)}{R_{HS}q}} \quad \text{(S6)}$$

where R_{HS} is the hard sphere repulsive radius; f_p is the volume fraction.

A constant was added in the background. More details could be found in the manual of SASfit.

Calculation of the structural parameters of the L_α phase

The lattice parameter (D) of the lamellar liquid crystalline phase is obtained according to the equations S7-S10, where d_{IL} and d_a are thickness of the solvent and solvophobic layer.

$$D = \frac{2\pi}{q_1} \quad \text{(S7)}$$

$$d_{IL} = D(1 - \Phi_a) \quad \text{(S8)}$$

$$d_a = \frac{D - d_s}{2} \quad \text{(S9)}$$

$$S = \frac{V_a}{2d_a} \quad \text{(S10)}$$

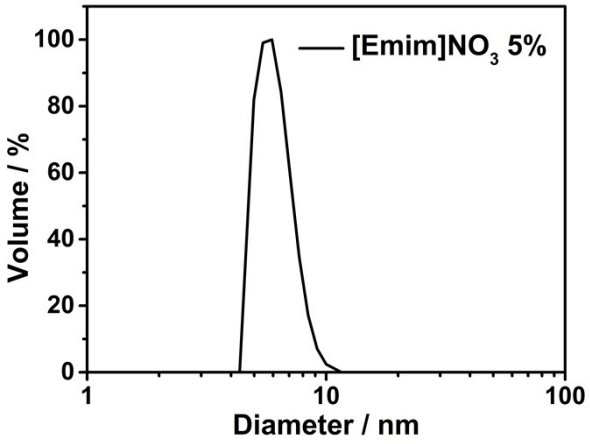

Fig. S2 Size distribution of aggregates in the 5% C_{16}mimBr/[Emim]$EtSO_4$ solution at 60°C.

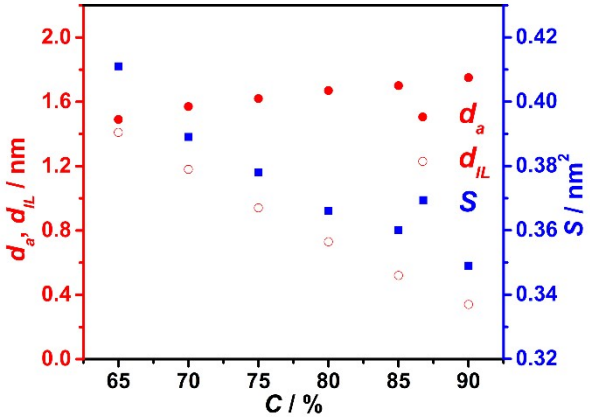

Fig. S3 Structure parameters of the L_α phases in the C_{16}mimBr/[Emim]NO_3 system at 60°C. d_a, solvophobic region thickness; d_{IL}, solvent layer thickness; S, the area occupied by the surfactant molecules at the solvophilic/solvophobic interface.

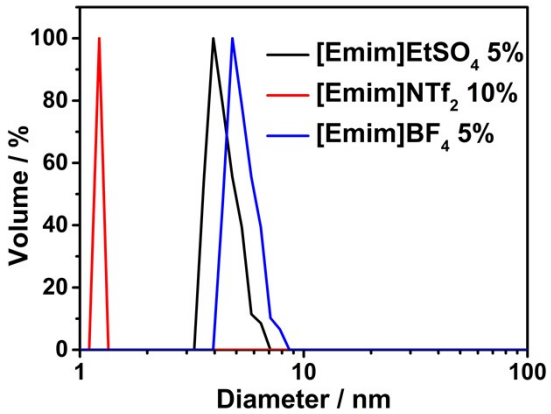

Fig. S4 Size distribution of aggregates in the C_{16}mimBr/AILs system at 60°C for different concentrations of C_{16}mimBr.

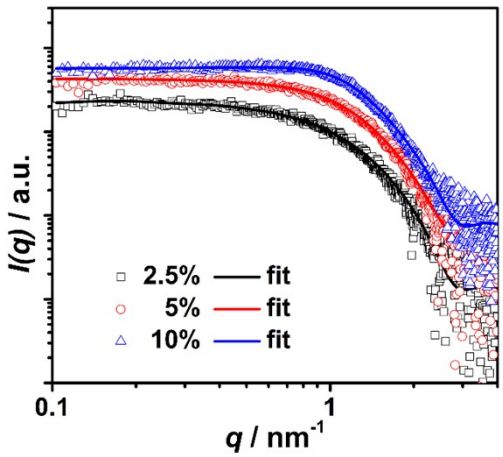

Fig. S5 SAXS patterns of micelles in the C_{16}mimBr/[Emim]$EtSO_4$ system at 60°C for different concentrations of C_{16}mimBr.

Table S1 Parameters of micelles in the C_{16}mimBr/[Emim]$EtSO_4$ system at 60 °C.

C / %	*a* / nm	*b* / nm	*ε*	*N*
2.5	1.43	3.04	2.12	57
5	1.42	3.67	2.59	68
10	1.40	2.92	2.09	52

a, the equal semi-axis; *b*, the principle semi-axis; *ε*, the axis ratio; *N*, the aggregation number.

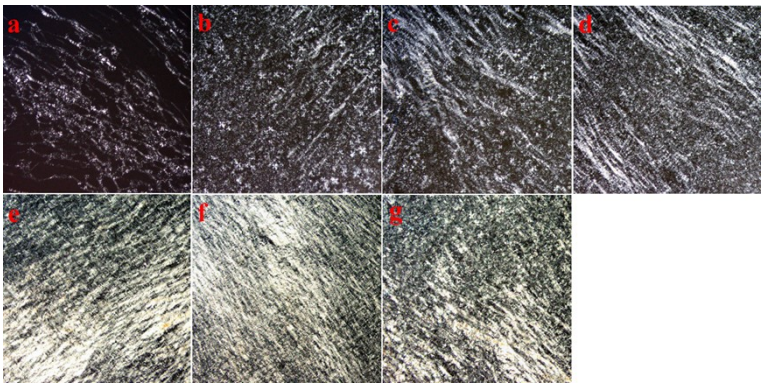

Fig. S6 POM images of the L_α phases in the C_{16}mimBr/[Emim]$EtSO_4$ system at 60°C. The C_{16}mimBr concentrations are 60 % (a), 65 % (b), 70 % (c), 75 % (d), 80 % (e), 85 % (f) and 90 % (g).

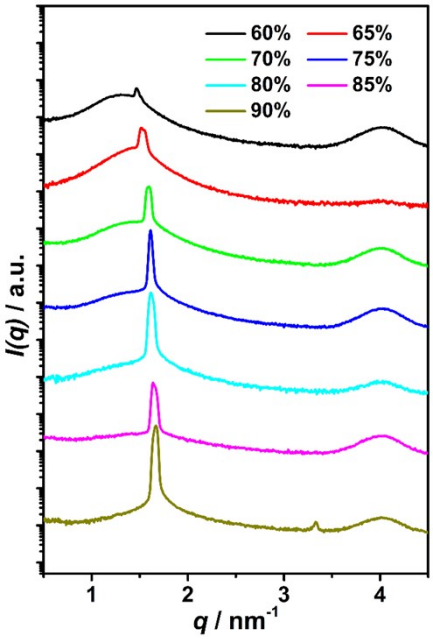

Fig. S7 SAXS patterns of the L_α phases in the C_{16}mimBr/[Emim]$EtSO_4$ system at 60°C for different concentrations of C_{16}mimBr.

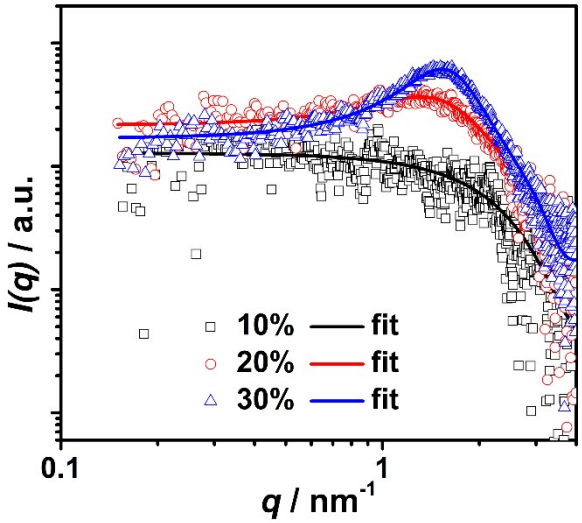

Fig. S8 SAXS patterns of micelles in the C_{16}mimBr/[Emim]NTf_2 system at 60°C for different concentrations of C_{16}mimBr.

Table S2 Parameters of micelles in the C_{16}mimBr/[Emim]NTf_2 system at 60°C.

C / %	*a* / nm	*b* / nm	*ε*	*N*
10	1.04	1.07	1.02	11
20	1.12	1.12	1.00	13
30	1.07	1.44	1.35	15

a, the equal semi-axis; *b*, the principle semi-axis; *ε*, the axis ratio; *N*, aggregation number.

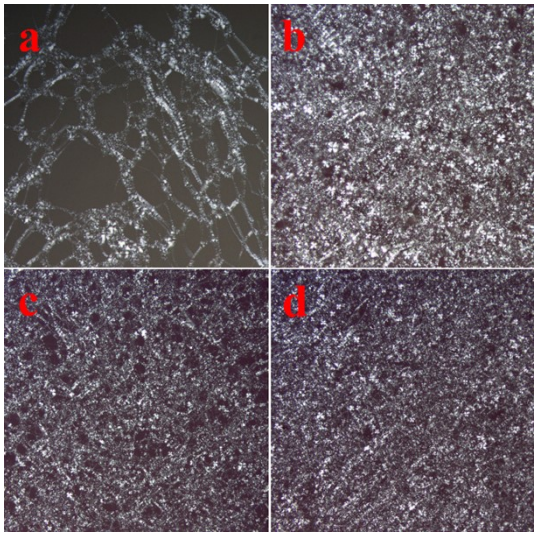

Fig. S9 POM images of the L_α phases in the C_{16}mimBr/[Emim]NTf_2 system at 60°C. The C_{16}mimBr concentrations are 70 % (a), 75 % (b), 80 % (c) and 85 % (d).

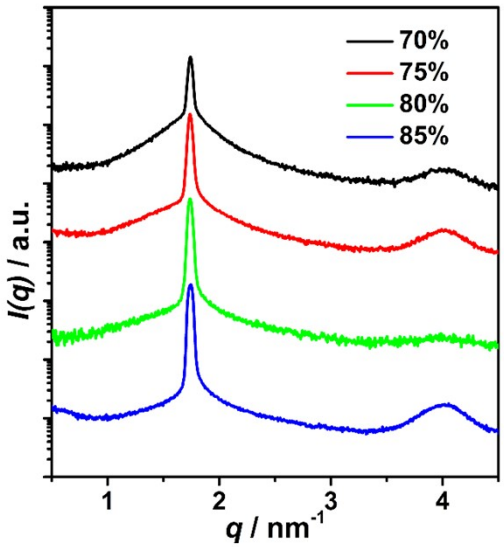

Fig. S10 SAXS patterns of the L_α phases in the C_{16}mimBr/[Emim]NTf_2 system at 60°C for different concentrations of C_{16}mimBr.

Table S3 CAC in the C_{16}mimBr/AILs system at 60°C.

AIL	X_M	$X_{L\alpha}$
[Emim]NO_3	0.0048	0.44
[Emim]$EtSO_4$	0.0096	0.47
[Emim]NTf_2	-	0.69

[Emim]BF_4	0.0047	0.52

X_M, CMC in the molar ratio; $X_{L\alpha}$, CAC of the L_α phase in the molar ratio.

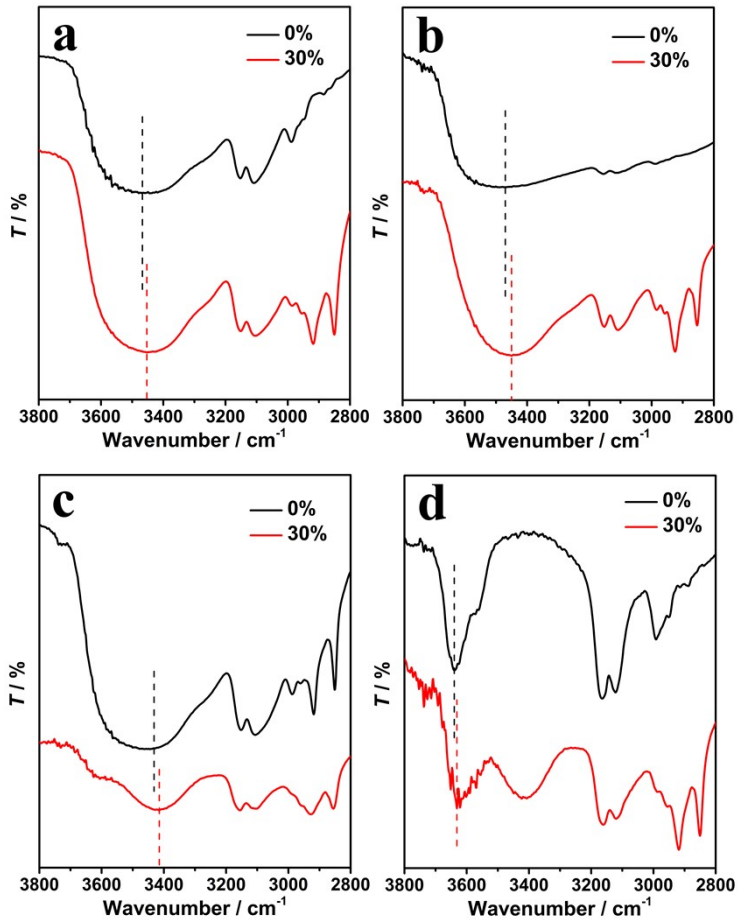

Fig. S11 FTIR spectra of AILs and 30 % C_{16}mimBr/AILs solutions.
(a) [Emim]NO_3; (b) [Emim]$EtSO_4$; (c) [Emim]NTf_2; (d) [Emim]BF_4.

Table S4 Rheology parameters of the 80 % C_{16}mimBr/AIL L_α phases at 60 °C.

AIL	*A*	*z*
[Emim]NO_3	2211	24.5
[Emim]$EtSO_4$	3136	29.9
[Emim]NTf_2	4695	29.7
[Emim]BF_4	2403	23.1

A, the number of flow units interacting with each other; *z*, the coordination number.

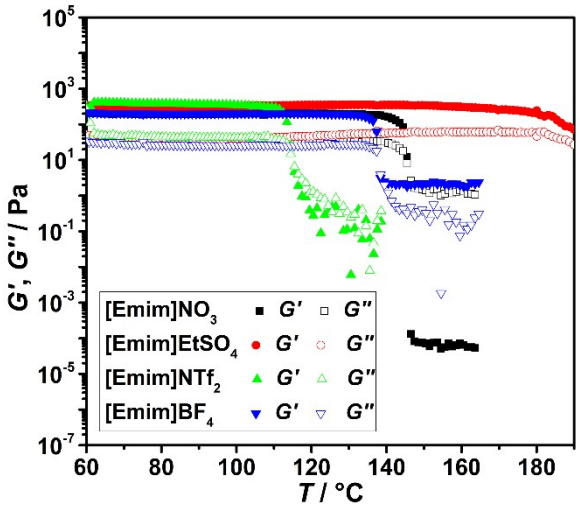

Fig. S12 Variations of *G′* and *G″* with temperature of the 80 % C_{16}mimBr/AIL L_α phases.

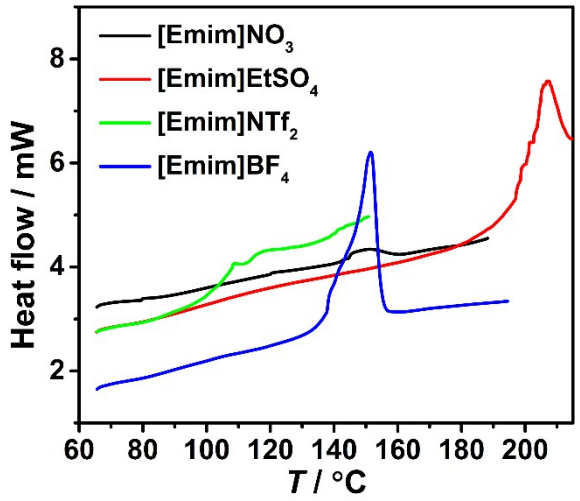

Fig. S13 DSC curves of the 80 % C_{16}mimBr/AIL L_α phases.

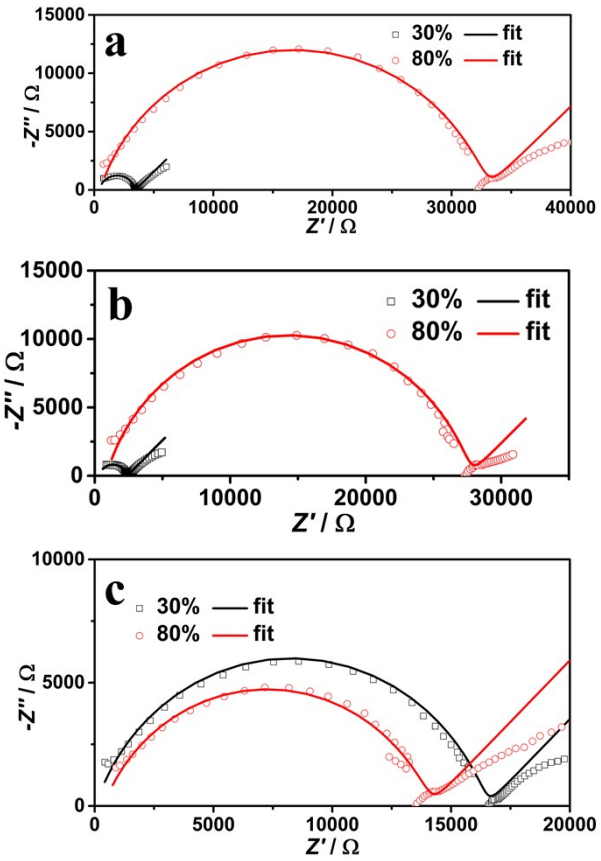

Fig. S14 EIS results of the L_1 and L_α phases in different AILs at 60°C. (a) $EmimNO_3$; (b) $EmimEtSO_4$; (c) $EmimBF_4$.

Table S5 Conductivity of the L_1 and L_α phases in different AILs at 60°C.

AIL	σ(AIL) / mS·cm^{-1}	σ(L_1, 30%) / mS·cm^{-1}	σ(L_α, 80%) / mS·cm^{-1}
$EmimNO_3$	18.6	0.331	0.0309
$EmimEtSO_4$	7.18	0.479	0.0373
$EmimBF_4$	21.6	0.0608	0.0476

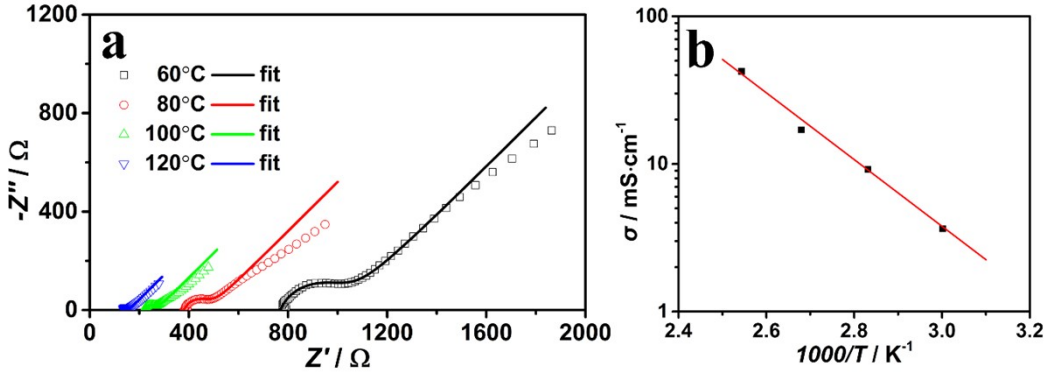

Fig. S15 EIS results (a) and conductivity (b) of the 80 % C_{16}mimBr/[Emim]NTf_2 L_α phase at different temperatures.